

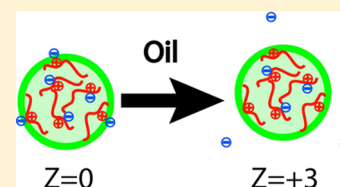
Charge Generation in Low-Polarity Solvents: Poly(ionic liquid)-Functionalized Particles

Ghulam Hussain, Amy Robinson, and Paul Bartlett*

School of Chemistry, University of Bristol, Bristol BS8 1TS, U.K.

Supporting Information

ABSTRACT: We present a straightforward strategy for the synthesis of highly charged poly(ionic liquid)-functionalized particles in low-polarity solvents. A series of cationic liquid monomers consisting of a tetraalkyl ammonium cation and a fluorinated tetrakis[phenyl] borate anion linked, via a C₃-alkyl chain, to a methacrylate unit were synthesized. The addition of this ionic monomer to a conventional dispersion polymerization of methyl methacrylate and methacrylic acid at 80 °C in a mixed dodecane/hexane solvent yielded spherical, highly monodisperse particles with mean diameters of between ~50 and 2500 nm with high electrophoretic mobility and stability in nonpolar solvents such as dodecane. The surface potential in dodecane could be adjusted in the range from 0 to 180 ± 9 mV by altering the ratio of ionic monomer to methacrylate monomers. The particles open up new opportunities for the electrostatic assembly of nanoparticles and organized structures in nonpolar environments.



1. INTRODUCTION

Electrostatics is a major driving force for self-assembly at the microscale and nanoscale.¹ Charge interactions play a crucial role in life and in many biological and industrial processes precisely because, at least in aqueous systems, they can be easily tuned. Forces can be attractive or repulsive and their magnitude and range can be controlled by altering the charge on the surfaces of interacting particles or the dielectric constant of the surrounding solvent or simply through adjustment of the concentrations of ions in solution. Anisotropic interactions may be generated by controlling surface geometry by, for instance, using charged cubes, rods, tetrahedra, or other 3D shapes^{1–3} or alternatively by chemically patterning the surface to produce heterogeneous charges.⁴ Although the vast majority of effort on nanoparticle electrostatics has focused quite naturally on aqueous systems, in recent years a growing interest has developed in nonaqueous “oily” solvents, those with dielectric constants of $\epsilon_{\text{oil}} \approx 2$. In this regime, some dissociation of charged groups does take place, although substantially less than in water, because the energetic costs of separating neutral species into free ions is larger by a factor of about $\epsilon_{\text{water}}/\epsilon_{\text{oil}} \approx 40$ in oil than in water. The synthesis possibilities offered by charge-directed self-assembly in nonpolar solvents have been most dramatically illustrated by the beautiful work on superlattice formation in mixtures of charged microparticles by the van Blaaderen group.⁵ This work sparked a new interest in the means to produce charge in low-dielectric solvents. Recent efforts have focused on either the fundamental nature of nanoscale electrostatics in the extremely low ion concentration environment (lower than nanomolar) found in low-dielectric solvents^{6–11} or on controlling particle charging,^{12–16} which is important in the commercial development of thin film electrophoretic particle displays (EPDs) and in the processing of petroleum products.^{17,18}

Microparticles are often charged in a low-polarity solvent by the addition of a suitable surfactant^{8,9,11–16} or what is sometimes called a charge-control additive.¹⁹ It is generally believed,

although not experimentally proven, that the nanometer-sized reverse micelles produced in situ by the surfactant solubilize counterions within their cores. The stabilization reduces the energy barrier to charge separation and so enhances the charge on the particle. The physical situation is, however, complex because the surfactant often plays two distinct roles. In addition to stabilizing ions, the surfactant frequently adsorbs onto the surface of the particle and generates new surface groups that then ionize. The total particle charge depends on a competition between the two processes of surface adsorption and bulk micellization. As a result, the particle charge is found experimentally to be sensitive to a large number of factors, among which the chemical nature and concentration of the surfactant, the surface functionality of the particle, the adsorption of the surfactant, the presence of water, and in some cases even the time of contact between surfactant and particle seem to be the major ones.^{8,9,11–16,19} So far, most efforts have been devoted to mapping out the consequences of this competitive surface chemistry so as to prepare particles with controlled levels of charge. Given these complexities, it would be highly desirable to develop a new family of particles that would charge spontaneously without surfactant. Adjusting the concentrations of surface groups would then allow the particle charge to be tailored precisely to a specific application. Furthermore, the absence of surfactant molecules should enhance chemical compatibility so that nanoparticles with different surface charges or polarities could be mixed together to self-assemble without the problems of charge exchange, which is such a detrimental feature of surfactant-based charging schemes. Although nonpolar asphaltene colloids, for example, have been shown recently to charge spontaneously in the absence of surfactants,^{17,18} no general synthesis method exists, as far

Received: December 12, 2012

Revised: February 8, 2013

Published: February 12, 2013

as we know, that permits the charge on a nanoparticle in a nonpolar environment to be controlled systematically and by design.

Polymerized ionic liquids (PILs) offer a potential new approach to the problems of nonpolar charging. PILs are a special type of polyelectrolytes that carry an ionic liquid (IL) functionality in each of their repeating units. In contrast to classical water-soluble polyelectrolytes, the IL functionality renders PILs soluble in organic solvents and insoluble in water. The family of PILs is very broad and includes organic cations such as dialkyl imidazolium, alkylpyridinium, and tetraalkyl-ammonium species and hydrophobic anions such as tetrafluoroborates (BF_4^-), hexafluorophosphates (PF_6^-), and fluorinated imides (such as $(\text{CF}_3\text{SO}_2)_2\text{N}^-$). Interest in PILs has expanded considerably in the past few years^{20,21} because they combine the unique versatility of ionic liquids with the design and control over architecture available in macromolecular systems and so offer opportunities for creating materials with new properties and functions. Although PILs have been exploited in applications as varied as ion-conductive electrolytes,^{22,23} stabilizing agents for carbon nanotubes and graphene,^{24,25} and carbon dioxide absorbents,²⁶ there seems to be no previous work on their use to generate charged particles in nonpolar environments.

In this Article, we construct ILs with polymerizable groups based on tetraalkyl-ammonium tetrakis[phenyl]borates and tetrakis[3,5-bis(trifluoromethyl)phenyl]borates. We utilize the hydrophobic nature of the cationic and anionic centers and the bulky size of the ions to reduce Coulombic interactions and enhance ion-pair dissociation in low-dielectric environments. The molecular architecture of the IL precursors was modified to maximize the ionic conductivity in nonpolar solvents such as dodecane and cyclohexane. Comparison with traditional surfactant-based approaches, using Aerosol-OT (AOT or sodium di-2-ethylhexylsulfosuccinate), for instance, shows that the ionic conductivity of the optimized IL precursors is 2 to 3 orders of magnitude greater than micellar surfactants in dodecane at the same molar concentration. The prepared IL monomers were mixed with methyl methacrylate and methacrylic acid and used in dispersion polymerization to prepare monodisperse poly(ionic liquid)-functionalized particles. Electrophoretic measurements demonstrate that the PIL-functionalized particles are highly charged in hydrophobic solvents such as dodecane. A preliminary report of this approach has already been published,²⁷ but in the present contribution, we report on our further efforts to optimize this system. In particular, we demonstrate that the surface potential of a polymer microparticle may be tuned continuously over a very wide range of values by altering the PIL content. Overall, our study shows that copolymerized PILs act efficiently as ionic groups in low-dielectric solvents, generate a high surface potential, and allow a high degree of control to be exercised over the particle charge.

2. EXPERIMENTAL SECTION

2.1. Materials. All reagents were purchased from Aldrich, Acros, or Alfa Aesar Chemicals and used in the synthesis procedures described below without significant further purification. All solvents used were of analytical grade. Poly(ionic liquid)-containing particles after synthesis were resuspended in hexane or dodecane, which were dried under nitrogen and stored in contact with 4 Å molecular sieves to minimize their water content prior to use.

2.2. Preparation of Ionic Liquid Precursors. Fluorinated tetraalkyl-ammonium tetrakis[3,5-bis(trifluoromethyl)phenyl]borates (compounds 1–5) and the analogous unfluorinated tetraalkyl-ammonium tetrakis[phenyl]borates (compounds 6–10) were prepared by anion exchange.²⁸ In a typical synthesis procedure, the quaternary ammonium bromide salt was dissolved in the minimum amount of methanol and then added to a methanolic solution of sodium tetrakis[3,5-bis(trifluoromethyl)phenyl]borate. The excess solvent was

evaporated, and the white precipitate that appeared was washed with diethyl ether and then recrystallized twice from acetone. The product was dried under vacuum. In the case of the tetraoctadecylammonium bromide, the solubility in methanol was low and the anion exchange was carried out in warm propanol. The structure of the product was confirmed by ^1H NMR, ^{13}C NMR, and microanalysis.

2.3. Preparation of Ionic Liquid Monomers. The synthesis of the ionic liquid monomers (ILMs) was accomplished using a three-step synthesis procedure illustrated for the $[\text{ILM-C}_{12}][\text{TFPhB}]$ monomer (13). In the first step, a hydroxyl-terminated *n*-tetraalkylammonium salt (11) was prepared by the quaternization of a tertiary amine with 3-bromo-1-propanol. In the next step, a methacryloyl group was introduced by reaction of the terminal hydroxyl group with methacryloyl chloride. The bromide anion was then exchanged with highly lipophilic anion tetrakis[3,5-bis(trifluoromethyl)phenyl]borate (TFPhB) to yield the desired product.

2.3.1. Synthesis of *n*-Tridodecyl-propyl-3-hydroxy Ammonium Bromide (11). Compound 11 was prepared by the Menschutkin reaction.²⁹ Tridodecylamine (10 mmol) and 3-bromo-1-propanol (11 mmol) were refluxed in DMF at 110 °C in the presence of the catalyst³⁰ dodecyl trimethyl ammonium bromide (DTAB, 1 mmol). ^1H NMR showed that quaternization was essentially complete after 24 h. The reaction mixture was cooled to room temperature, and 100 mL of ice-cold diethyl ether was added. The precipitate was washed thoroughly with further diethyl ether and recrystallized from an equal volume mixture of ethyl acetate and methanol.

2.3.2. Synthesis of *n*-Tridodecyl-propyl-3-methacryloyloxy Ammonium Bromide (12). One millimole of 11 was loaded into a 50 mL reactor under nitrogen in the presence of 2.5 mmol of triethylamine in dichloromethane. The mixture was cooled by an ice bath. Three millimoles of methacryloyl chloride was added dropwise over a hour with vigorous stirring. The resulting mixture was poured into water (100 mL) and extracted with diethyl ether twice. The organic extracts were filtered and concentrated in vacuo to yield a white precipitate.

2.3.3. Synthesis of $[\text{ILM-C}_{12}][\text{TFPhB}]$ Monomer (13). A solution of sodium tetrakis[3,5-bis(trifluoromethyl)phenyl]borate (Na-TFPhB) (1 mmol) in 10 mL of methanol was added dropwise to a solution of 12 in methanol at 0 °C. After a hour, an excess of ice-cold distilled water was added. The precipitate was extracted with diethyl ether and concentrated in vacuo. The residue was purified by flash column chromatography on silica gel and eluted with 0 to 5% methanol in a 1:1 (v/v) mixture of dichloromethane and hexane.

2.4. Polymerization Process. Dispersion polymerizations of methyl methacrylate (MMA), methacrylic acid (MA), and ILM were carried out in a mixed solvent of hexane and dodecane at 80 °C under nitrogen following the procedure detailed by Antl et al.³¹ 2,2'-Azobis(isobutyronitrile) (AIBN) and a comb copolymer, poly(12-hydroxy stearic acid)-*co*-poly(methyl methacrylate) (P(HSA-*co*-MMA)), were used as the initiator and stabilizer, respectively. Chain-transfer agent 1-octanethiol (OT) was added to limit the polymer molecular weight. The weight percentage of the ionic monomer (ILM) was varied from between 0 and 8% of the masses of the MMA and MA monomers, as detailed in Table 1. The total mass of

Table 1. Typical Recipe for the Preparation of PIL-Containing Particles

ingredients	mass (g)
[ILM]	0.4 ^a
[MMA]	4.9
[MA]	0.1
[P(HSA- <i>co</i> -MMA)] ^b	0.83
[AIBN]	0.04
[OT]	0.03
[dodecane]	0.98
[hexane]	3.12

^aVaried between 0.0 g (0% ILM) and 0.4 g (8% ILM). ^b30% by weight solution in dodecane.

MMA and MA monomers was fixed at 50% of the total weight of the preparation. After 2 h, the comb stabilizer was chemically bound to the surfaces of the particles by raising the temperature to 120 °C in the presence

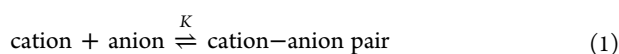
of catalyst diethanol amine (0.025 g). After being refluxed for 8 h, the cooled suspension was then passed through tightly packed glass wool to remove coagulant and cleaned by five repeated cycles of centrifugation and redispersal in fresh hexane before use.

2.5. Characterization Methods. NMR spectra were recorded at room temperature using a Varian 400-MR spectrometer operating at 400 MHz for ^1H spectra and 101 MHz for ^{13}C spectra. The average radius $\langle a \rangle$ of the poly(ionic liquid) particles and their coefficient of variation $C_v = (\langle a^2 \rangle - \langle a \rangle^2)^{1/2} / \langle a \rangle$ were determined from scanning electron microscopy (SEM, JEOL JSM-5600LV, Jeol Ltd., U.K.). A drop of each dispersion was diluted in a few milliliters of pure hexane and then deposited on a glass coverslip attached to an aluminum stub with conductive glue. The sample was dried at room temperature in an enclosed cabinet before sputter coating with gold. Five images, containing about 250 particles each, were collected and measured using image analysis software (Vision Assistant, National Instruments). The hydrodynamic radius a_h was determined by dynamic light scattering (DLS) from dilute suspensions (0.006 to 0.01 wt %) in dodecane using a Malvern Instruments system (Zetasizer Nano Series S, Malvern Instruments, U.K.). Electrophoretic mobilities μ were determined using a combined laser Doppler velocimetry and phase analysis light scattering (M3-PALS) technique (Zetasizer Nano Series Z, Malvern Instruments, U.K.). Particles were driven with an ac electric field of $2 \times 10^4 \text{ V m}^{-1}$, and the particle velocity was determined from the phase shift of the scattered laser light. Measurements were made at 25°C on dilute dispersions (0.006 wt %, colloid volume fraction $\eta_c = 3.8 \times 10^{-5}$) in dry filtered dodecane. No appreciable variation of μ with field strength was detected for field strengths from between $2 \times 10^4 \text{ V m}^{-1}$ and $6 \times 10^4 \text{ V m}^{-1}$; however, systematic measurements to investigate a wider range of electric fields are currently planned. For each particle sample, at least 20 runs, each consisting of 100 individual measurements, were recorded to ensure the accuracy of the results. The conductivity of electrolyte solutions in cyclohexane was measured at an ac frequency of 18 Hz and 25°C using a Scientifica (U.K.) model 627 conductivity meter.

3. THEORY

3.1. Ion Pairing. To detail the interactions between ions in a low-polarity solvent, we use the quasi-chemical ion pairing approach pioneered by Bjerrum,³² which gives excellent agreement with Monte Carlo simulations³³ of associating ionic fluids at the very low concentrations relevant here. For completeness, we summarize the key features below for a dilute 1:1 electrolyte and refer the interested reader to the recent presentation of Valeriani et al.³³ for a more detailed analysis.

In the low-dielectric-constant solvents studied here, the ion concentrations are very small, typically less than 10^{-9} M , so triple ions and other highly charged clusters may be safely ignored. Bjerrum's theory assumes that a dynamic equilibrium exists between free ions and the bound ion pairs in solution.



In terms of α , the fraction of salt molecules that are dissociated into free ions, and ρ_s , the total number density of salt molecules, the number densities of cations $\rho_+ = \alpha\rho_s$, anions $\rho_- = \alpha\rho_s$, and ion pairs are $\rho_{\text{IP}} = (1 - \alpha)\rho_s$. The molar salt concentration is accordingly $c_s = \rho_s/N_A$, where N_A is Avogadro's constant and $\rho_s = 1/2(\rho_+ + \rho_-) + \rho_{\text{IP}}$. (Note that the maximum ion concentration is actually $2c_s$ when all ion pairs are completely dissociated.) Applying the law of mass action to eq 1 yields

$$K\rho_s = \frac{1 - \alpha}{\alpha^2} \quad (2)$$

Here, K is the ion-pair association constant. Solving eq 2 for α gives

$$\alpha = \frac{1}{2K\rho_s} (\sqrt{1 + 4K\rho_s} - 1) \quad (3)$$

At low salt concentrations, eq 3 shows that, for $K\rho_s \ll 1$, all ion pairs are almost completely dissociated ($\alpha \approx 1$) as a result of the favorable gain in entropy on dissociation. By contrast, at high salt concentrations, where $K\rho_s \gg 1$, the entropy of mixing is less important in comparison to the ion-pair binding energy, and the majority of ions remain bound as ion pairs with $\alpha \approx 1/(K\rho_s)^{1/2}$. The dividing boundary between the dissociated and associated regimes may be identified with the line $K\rho_s = 2$, where $\alpha = 1/2$.

The equilibrium constant K may be extracted from experimental measurements of the conductivity S . If the mixture of cations, anions, and cation-anion pairs is sufficiently dilute to be ideal, then the conductivity is

$$S = \left(\frac{\rho_+}{N_A} \right) \Lambda_+ + \left(\frac{\rho_-}{N_A} \right) \Lambda_- + S_0 \quad (4)$$

where Λ_+ (Λ_-) is the molar conductivity of the cation (anion) at infinite dilution and S_0 is the background conductivity of the solvent. For a 1:1 electrolyte, the total molar conductivity Λ_0 is just the sum of the contributions from each ion, so $\Lambda_0 = \Lambda_+ + \Lambda_-$. By replacing the equilibrium constant K by the dimensionless molar ion-pairing constant $K_M = KN_A c^\circ$, where the standard concentration is $c^\circ = 1 \text{ mol m}^{-3}$, and using the expression for α from eq 3, the conductivity may be re-expressed in a form convenient for data analysis,

$$S = \frac{\Lambda_0 c_0}{2K_M} \left(\sqrt{1 + 4K_M \left(\frac{c_s}{c_0} \right)} - 1 \right) + S_0 \quad (5)$$

The association of ions in low-dielectric solvents is dominated by the long-range Coulombic interactions between ions. The details of the short-range repulsive interactions and the attractive van der Waals interactions between ions, which are a function of their precise chemistry, are believed to be much less important than an accurate modeling of the electrostatic forces.³⁴ To interpret the measured ion association constants, we use a restricted primitive model (RPM) of the ionic fluid. This model assumes spherical hard ions of unit positive and negative charge and equal diameter d in a solvent, which is regarded as a dielectric continuum of dielectric permittivity $\epsilon_r \epsilon_0$. The hard-sphere ions interact only via pairwise additive Coulombic interactions. The electrostatic binding energy $U_c/k_B T$ at contact between oppositely charged ions is defined conveniently as λ_B/d (in units of $k_B T$), where the Bjerrum length λ_B is

$$\lambda_B = \frac{e^2}{4\pi\epsilon_0\epsilon_r k_B T} \quad (6)$$

Experimental data may be converted into equivalent RPM units by determining an effective hard-sphere diameter d_{RPM} that reproduces the measured association constant K_M . An approximate closed-form expression for $K = K_M/(N_A c^\circ)$, valid at the large ion-pair binding energies $U_c/k_B T \gg 25$ appropriate to this study, has been given for the restricted primitive model by Valeriani et al.³³

$$K = 4\pi d^3 e^{\lambda_B/d} \left[\frac{d}{\lambda_B} + 2 \left(\frac{d}{\lambda_B} \right)^2 + 2 \left(\frac{d}{\lambda_B} \right)^3 \right] \quad (7)$$

The effective hard-sphere diameter d_{RPM} is obtained by equating the experimentally determined values of the ion-pair association constant K with the expression in eq 7. The ion diameter d_{RPM} is obtained by a numerical solution of eq 7 using the known λ_B .

3.2. Electrokinetics in Counterion-Free Systems. When a colloidal particle of radius a containing a large number of ionizable

poly(ionic liquid) groups at its surface is immersed in a low-dielectric solvent, some of the ionizable groups dissociate, releasing counterions into the solution and leaving opposite charges on the surface. Because of the dissociation of surface groups, the colloidal surface acquires a net surface charge density of $e\sigma$ that is assumed to be distributed homogeneously over the surface. Poisson–Boltzmann (PB) theory, which ignores ion–ion correlations, provides an extremely convenient description of the ion distribution outside such a charged colloidal particle. For monovalent ions, the mean-field picture that underlies the PB theory is accurate provided that the dimensionless coupling constant $\Xi = 2\pi\sigma\lambda_B^2 < 1$. This weak coupling condition equates to a surface charge density of approximately 1 elementary charge per 10 square Bjerrum lengths.³⁵ As we will see later, this condition is satisfied in the nonpolar suspensions relevant here, where maximum charge densities are on the order of 1e per 100 square Bjerrum lengths, so PB theory should provide an accurate description of the ion distribution in a low-polarity solvent.

The electrophoretic mobility $\mu = v/E$, defined by the ratio of the colloid drift velocity v to the applied electric field E , of a spherical charged colloidal particle immersed in an electrolyte solution has been extensively studied within the framework of a PB approach. In the common salt-dominated regime, the large reservoir of salt ions results in a strong screening of the equilibrium electrostatic potential $\phi(r)$ (where r is the distance from the center of the particle) so that the space charge density is essentially zero throughout the solution, except for within a narrow ionic atmosphere (the “Debye cloud”) surrounding each colloid. Because the bulk solution phase is electroneutral, an applied electric field exerts forces only on the particle and its Debye layer. The hydrodynamic interactions between particles subject to electrophoresis are therefore strongly screened and the mobility μ is essentially constant, being only weakly dependent on the particle concentration.³⁶ The situation becomes very different in the much less frequently studied counterion-dominated regime. Here the intervening solution between charged particles contains only counterions, which are ions of one charge sign generated by the dissociation of colloid surface groups. There is no bulk ion reservoir, so the space charge density in the solution cannot become zero, even far from the particle surface. Screening is reduced, and the dependence of μ on the particle concentration is now found to be significant. The different electrokinetic phenomena in the counterion- and salt-dominated regimes have been explored theoretically by Ohshima^{37–39} and others.^{40–42} Here we briefly review the counterion-only model of electrophoresis that we use to interpret our experimental data.

We assume that the colloids are positively charged and that the only ions present in the bulk of the solution are the negative counterions. To allow a straightforward numerical solution of the nonlinear Poisson–Boltzmann equation, a cell model first proposed by Alexander et al. is used.⁴³ A suspension of N charged spheres is approximated by N identical spherical Wigner–Seitz (WS) cells of radius R , each containing a single colloid of charge $+Ze$ at the center and surrounded by Z negative monovalent counterions such that the cell is overall electrically neutral. The cell radius R is chosen such that $\eta_c = (a/R)^3$ equals the volume fraction occupied by the colloidal particles. Let $\Phi(r) = e\phi(r)/k_B T$ be the reduced electrostatic potential a distance r from the center of the colloid. Then in a mean-field approximation the potential $\Phi(r)$ inside the cell ($a \leq r \leq R$) is the solution of the nonlinear PB equation,

$$\frac{d^2\Phi}{dr^2} + \frac{2}{r} \frac{d\Phi}{dr} = \gamma^2 e^{\Phi} \quad (8)$$

where γ is a prefactor whose value is fixed by the electroneutrality constraint. The prefactor γ plays a role analogous to that of the

Debye screening parameter κ in the case with added electrolyte, although in the absence of a salt reservoir κ is strictly undefined.⁴⁴ The counterion density in the WS cell is $\rho_-(r) = \rho_0 e^{\Phi}$, where ρ_0 is the average number density of counterions³⁸ chosen so that the neutrality condition $Z = 3/4\pi(R^3 - a^3)\rho_0$ is satisfied. In terms of ρ_0 , the prefactor γ satisfies the equality $\gamma^2 = 4\pi\lambda_B\rho_0$ that can be rearranged to give

$$(\gamma a)^2 = 3 \frac{Z\lambda_B}{a} \left(\frac{\eta_c}{1 - \eta_c} \right) \quad (9)$$

The boundary conditions are, at the colloid surface,

$$r \frac{d\Phi}{dr} \Big|_{r=a} = -\frac{Z\lambda_B}{a} \quad (10)$$

and through electroneutrality, at the cell boundary,

$$\frac{d\Phi}{dr} \Big|_{r=R} = 0 \quad (11)$$

The system of differential and algebraic equations (eq 8–11) is solved numerically by the elegant algorithm proposed in ref 44. The potential drops rapidly in the vicinity of the particle surface from $\Phi_s = \Phi(a)$ before going negative and reaching a finite negative value of $\Phi_o = \Phi(R)$ at the edge of the WS cell. The total potential difference from the surface of the particle to the boundary of the WS cell is $\Phi_d = \Phi_s - \Phi_o$.

An expression for the electrophoretic mobility μ of a spherical colloidal particle in a salt-free suspension has been derived under the condition of a weak applied electric field by Ohshima.^{37,39,45} The analytical result was obtained by approximating the exact electrokinetic equations of motion for dilute particle concentrations ($\eta_c \ll 1$). More sophisticated numerical calculations on cell models^{41,42} confirm the validity of these approximations whereas recent mesoscopic⁴⁶ and lattice Boltzmann simulations⁴⁰ show that the electrophoretic response of salt-free systems is indeed captured reasonably well by the analytical predictions of Ohshima. The mobility was obtained by balancing the Stokes drag force on the uncharged particle with the pressure from the excess counterion charges on the boundary of the WS cell. In the dilute limit $\eta_c \ll 1$, the result is³⁷

$$\mu = \frac{Ze}{6\pi\eta a} \Omega \exp(\Phi_o) \quad (12)$$

with

$$\Omega = 1 - \frac{9\eta_c^{1/3}}{5} + \eta_c - \frac{\eta_c^2}{5} \quad (13)$$

In the low-charge (or low surface potential) limit, where the potential at the outer boundary of the cell approaches zero, eq 12 reduces to the conventional Hückel equation. Increasing the particle charge Z (or surface potential Φ_s) increases the retardation due to the enhanced counterion density at the boundary of the cell, which in turn reduces the magnitude of the electrophoretic mobility. By introducing the dimensionless mobility μ^* ,

$$\mu^* = \frac{6\pi\eta\lambda_B}{e} \mu \quad (14)$$

eq 12 may be rewritten as

$$\mu^* = \frac{Z\lambda_B}{a} \Omega \exp(\Phi_o) \quad (15)$$

Accurate values of μ^* were obtained from a numerical solution of the Poisson–Boltzmann equation (eq 8).

4. RESULTS AND DISCUSSION

4.1. Selection of IL Precursors. Since the late 1990s, the group of Ohno²³ has devoted considerable efforts to the synthesis of PILs via free radical polymerization of suitable monomers with the goal of preparing a solid ionic electrolyte for batteries. The IL monomers used typically contain a cation fixed into the main chain of the unit, polymerizable methacryloyl or *N*-vinylimidazolium groups, and a suitable anion. Methacryloyl-based IL monomers, in particular, offer versatility because they may be readily copolymerized with other monomers to tune ion-conductive properties. Ohno et al. has systematically studied the relationship between molecular structure and the resulting solid-state ionic conductivities.²³ Key structural parameters were identified to be the nature of the anion, the length of the spacer group between the polymerizable group and the cation (for methacryloyl-based monomers), and the length of alkyl chains attached to the cation center. Although in the current work we are aiming for solution rather than solid-state properties, the approach of Ohno et al. provides a natural starting point for optimization. Our synthesis strategy was therefore to prepare methacryloyl-based monomers with a long-chain tetraalkyl ammonium cation separated from the polymerizable group by a short flexible C₃-alkyl chain, chosen to improve ionic conductivity.^{23,47} The nature of the counteranion is known to have a strong influence on the solubility behavior of cationic PILs.²⁰ Abbott et al. have reported^{28,48} that quaternary ammonium salts with carbon chains greater than C₈ show surprisingly high solubilities in cyclohexane and supercritical carbon dioxide, particularly when combined with tetraphenylborate anions. For instance, the hydrophobic species tetrakis(decyl) ammonium tetraphenylborate has a solubility of approximately 0.045 mol dm⁻³ in cyclohexane at room temperature, and the solubility may be increased still further by using fluorinated hydrophobic anion tetrakis[3,5-bis(trifluoromethyl) phenyl]borate [TFPhB].

We chose to investigate the family of ionic liquid precursors, compounds 1–10, that are characterized by two structural features: (1) a tetraalkyl ammonium unit containing a C_{*n*} chain and (2) counterions of either tetrakis[phenyl]borate [TPhB]⁻ or the more hydrophobic species tetrakis[3,5-bis(trifluoromethyl)phenyl]borate [TFPhB]⁻. To optimize the ionization of the IL precursors in low-polarity solvents, we altered both the length *n* of the carbon chain in the cation and the nature of the counterion. The degree of ionization was determined from the measured conductivity of dilute solutions (*c*_s = 0.1–100 μM) of the ILs in cyclohexane ($\epsilon = 2.02$) using the expressions outlined in section 3.1.

The strong influence of the counteranion is clearly seen in the solubility behavior in low-polarity solvents such as cyclohexane. When a tetrakis[phenyl]borate anion and a tetraalkylammonium [H(CH₂)_{*n*}]₄N⁺ cation of the materials synthesized (*n* = 4, 6, 8, 12, and 18) were used, only the C₁₂ version of the compound was soluble in cyclohexane. However, when the [TPhB]⁻ anion was replaced with the fluorinated species [TFPhB]⁻, all of the different chain length compounds readily dissolved in cyclohexane. The dramatic effect of fluorination is evident in the ionic conductivity, plotted in Figure 1. Although both the fluorinated and nonfluorinated ionic liquids offer higher conductivities than conventional surfactant systems,¹⁴ the fluorinated anion produces a substantial increase in the number of ions, with an ionic conductivity that is about 10 times higher at a salt concentration of *c*_s = 1 μM. The performance increase, however,

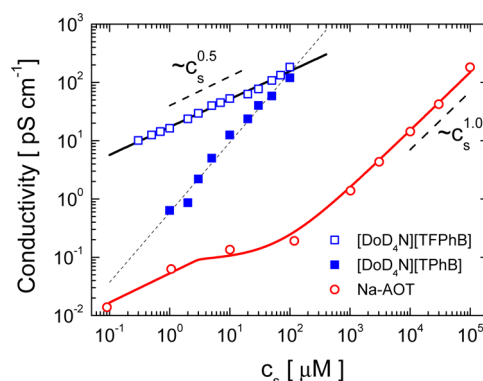


Figure 1. Conductivity (in cyclohexane) as a function of molar concentration for the fluorinated IL [DoD₄N][TFPhB] and the unfluorinated IL [DoD₄N][TPhB]. For comparison, the conductivity of Na-AOT in dodecane¹⁴ at 25 °C is also shown. The solid curve (black) through the [DoD₄N][TFPhB] data is the prediction of eq 5, while the line (red) through the AOT data is calculated for a critical micellar concentrations of 3 μM. The [DoD₄N][TPhB] data, which shows an approximate linear dependence on electrolyte concentration (dashed line), cannot be fitted with eq 5.

decreases with increasing *c*_s because the conductivity of [DoD₄N][TPhB] increases more markedly than that of the [DoD₄N][TFPhB] solution with increasing concentration. Although the [DoD₄N][TFPhB] system shows the square-root dependence expected for a weak electrolyte, the nearly linear dependence on *c*_s seen for [DoD₄N][TPhB] clearly points to a different mechanism of charging in the nonfluorinated system. Symmetric tetra-alkyl ammonium cations are known to be surface-active,⁴⁹ so we postulate that the [DoD₄N][TPhB] solution contain micelles in addition to associated molecular ions. A micellar disproportionation mechanism, analogous to that identified in Na-AOT,⁵⁰ would account for the linear dependence of conductivity on *c*_s observed. However, because the unfluorinated system was only sparingly soluble in nonpolar solvent we did no further work to prove these speculations and focused solely on the fluorinated system.

The length (*n*) of the alkyl chain substituent on the quaternary ammonium cation [H(CH₂)_{*n*}]₄N⁺ has a dramatic effect on the conductivity and solubility of the fluorinated salts. Increasing the carbon chain length from C₄ to C₁₂ led to a nearly 40-fold increase in the conductivity in cyclohexane (Figure 2). The C₁₂ species, however, had the maximum conductivity of all of the C_{*n*} compounds studied (*n* = 4, 6, 8, 12, and 18), with the C₁₈ compound being only sparingly soluble in cyclohexane. To relate these changes to the change in the Coulombic interactions, the conductivity data for the fluorinated salts was analyzed quantitatively using the ion-pairing theory detailed in section 3.1. The conductivity *S* was fitted to eq 5, with the dimensionless ion-pairing association constant *K*_M as a fitting parameter. The predicted conductivities, shown as the solid lines in Figure 2, will reproduce the experimental dependence of *S* on the salt concentration. The limiting molar conductivity at infinite dilution $\Lambda_0 = \Lambda_+ + \Lambda_-$ was calculated from *r*_±, the radii of the ions, using the expression⁵¹ $\Lambda_{\pm} = N_A e^2 / (6\pi\eta r_{\pm})$, where η is the viscosity of the solvent. The radius of the cation *r*₊ was estimated from the van der Waals volume *V*_{vdw} of the isolated ion, $r_+ = [(3/4\pi N_A)V_{vdw}]^{1/3}$, using the group contributions tabulated by Marcus.³⁴ The anion radius was taken from the literature.⁴⁸ The resulting values are summarized in Table 2. The fitted values of *K*_M are reported in Table 3, with, as expected, the highest association constant being

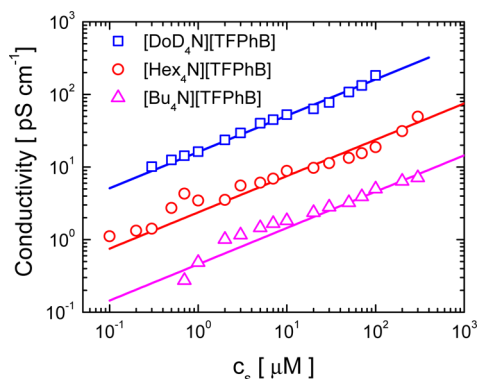


Figure 2. Conductivity as a function of salt concentration for $[\text{Bu}_4\text{N}][\text{TFPhB}]$, $[\text{Hex}_4\text{N}][\text{TFPhB}]$, and $[\text{Dod}_4\text{N}][\text{TFPhB}]$ in cyclohexane at 25 °C. The solid curves are the theoretical predictions of eq 5 using the ion-pairing association constants K_M listed in Table 3.

Table 2. Physical Parameters of Long-Chain Tetra- n -alkylammonium Salts in Cyclohexane

salt	n	r_+ (Å) ^a	r_- (Å) ^b	Λ_+ (S cm ² mol ⁻¹)	Λ_- (S cm ² mol ⁻¹)
$[\text{Bu}_4\text{N}][\text{TFPhB}]$	4	4.13	4.40	22.2	20.8
$[\text{Hex}_4\text{N}][\text{TFPhB}]$	6	4.68	4.40	19.6	20.8
$[\text{Oct}_4\text{N}][\text{TFPhB}]$	8	5.13	4.40	17.9	20.8
$[\text{Dod}_4\text{N}][\text{TFPhB}]$	12	5.85	4.40	15.7	20.8
$[\text{OD}_4\text{N}][\text{TFPhB}]$	18	6.67	4.40	13.7	20.8

^aCation radius estimated from van der Waals volumes.³⁴ ^bAnion radius from Abbott et al.⁴⁸

Table 3. Conductivity of Long-Chain Tetra- n -alkylammonium Salts in Cyclohexane at 25 °C

salt	n	K_M ^a	d_{RPM}^b (Å)	$Uc/k_B T^c$	c_{ion} (nM) ^d
$[\text{Bu}_4\text{N}][\text{TFPhB}]$	4	8.8×10^{12}	7.0	39.4	0.003–0.11
$[\text{Hex}_4\text{N}][\text{TFPhB}]$	6	6.29×10^{11}	7.8	35.5	0.019–0.59
$[\text{Oct}_4\text{N}][\text{TFPhB}]$	8	8.61×10^{10}	8.2	33.8	0.041–1.28
$[\text{Dod}_4\text{N}][\text{TFPhB}]$	12	5.1×10^9	8.9	30.9	0.140–4.41
$[\text{OD}_4\text{N}][\text{TFPhB}]^e$	18				

^aDimensionless ion-pair association constant determined from conductivity data. ^bEquivalent RPM hard-sphere diameter determined from eq 7 with $\lambda_B = 27.7$ nm. ^cIon-pair binding energy. ^dIon concentration $c_{\text{ion}} = (\rho_+ + \rho_-)/N_A$ determined for salt concentrations of $c_s = 0.1$ and 100 μM . ^eThe octyldecyl salt was insoluble in cyclohexane.

found for the soluble tetraalkyl ammonium salt with the smallest cation where the Coulombic interactions are maximized.

To understand quantitatively the strength of the association between IL ions in a low-polarity solvent, we map the fitted values of K_M onto an equivalent restricted primitive model (RPM) of the ionic fluid using the approach of Valeriani et al.³³ An effective ion diameter d_{RPM} was determined by equating the experimental values for K with the asymptotic RPM expression given in eq 7. The results are summarized in Table 3. To gauge the validity of an RPM description, the diameter difference $\Delta = (r_+ + r_-) - d_{\text{RPM}}$ between the van der Waals diameter and the RPM ion diameter is plotted in Figure 3 as a function of the alkyl chain length n . Because the restricted primitive model considers only Coulombic interactions and ignores both the precise details of the short-range repulsive interactions and any long-range van der

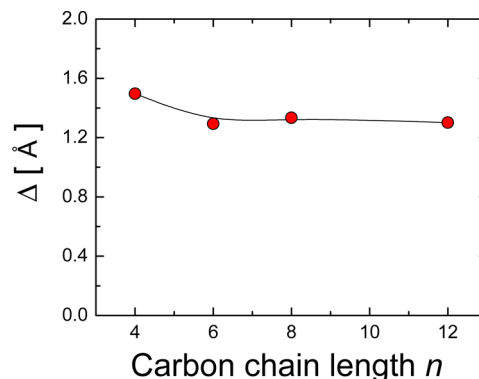


Figure 3. Difference between the van der Waals diameter and the restricted primitive diameter for $[\text{H}(\text{CH}_2)_n]_4\text{N}^+[\text{TFPhB}]^-$ as a function of n .

Waals attractions between ions, the values of Δ are unlikely to be exactly zero. Nonetheless, the data in Figure 3 reveals that Δ is first a relatively small fraction (between 12 and 18%) of the ion diameter and second rather unexpectedly almost constant at $\Delta \approx 1.3$ Å, independent of the alkyl chain length. The central conclusion is that the restricted primitive model gives a surprisingly accurate description of the ion-pairing association of tetra-alkyl ammonium salts in a low-polarity solvent. Within the RPM, the Coulombic interaction between ions at contact is $U_c/k_B T = \lambda_B/d_{\text{RPM}}$. The derived values are reported in Table 3. Although the binding energies are substantial, the fraction of dissociated ions is still larger than for surfactant systems typically used in nonpolar solvents. For instance, at a solute concentration of $c_s = 0.1$ μM more than 1 in 10^3 molecules in the $[\text{Dod}_4\text{N}][\text{TFPhB}]$ system are ionized compared to less than approximately 1 in 10^6 micelles in a surfactant system.⁹

4.2. Synthesis of Ionic Liquid Monomers (ILMs). Having identified $[\text{Hex}_4\text{N}][\text{TFPhB}]$ and $[\text{Dod}_4\text{N}][\text{TFPhB}]$ as the two most conductive combinations, we introduced these moieties into two methacrylic monomers, $[\text{ILM-C}_6][\text{TFPhB}]$ and $[\text{ILM-C}_{12}][\text{TFPhB}]$. The cations were incorporated into the backbone of the monomer, and the anion was left free to dissociate. The full details of the synthesis procedure used to prepare the cationic monomers are contained in section 2.3, but essentially a methacryloyl functional group was introduced, separated from the cationic C_6 - and C_{12} -alkyl substituted ammonium cation by a short three-carbon spacer chain. Ohno et al. has shown^{23,47,52} that the length of this spacer group has an important influence on the solid-state ionic conductivity in the case of the analogous polyelectrolyte, poly[2-alkyl imidazolium bis(trifluoromethanesulfonyl)imide]. With too short a spacer, the ionic conductivity drops precipitously, whereas for spacer groups of C_3 or larger the conductivity increases. The dependence on the alkyl chain length was relatively weak for $n \geq 3$, so in the present work we used a fixed C_3 spacer.

4.3. Preparation of PIL-Containing Particles by Dispersion Polymerization. The ILMs were used as a comonomer in a conventional dispersion polymerization of poly(methyl methacrylate) particles at 80 °C in a mixed solvent of dodecane and hexane with 2.5 wt % poly(12-hydroxy stearic acid-co-poly(methyl methacrylate) (P(HSA-co-MMA)) as a stabilizer. Thermal initiator 2,2'-azobis(isobutyronitrile) (AIBN) was used. The ILM was mixed with a fixed weight of methyl methacrylate (MMA) and methacrylic acid (MA) chosen so that before any addition of ILM the reaction mixture contained 50 wt % monomer. To control the particle charge, the proportion of ILM was varied from between 0 to 8 wt % (based on the mass of the non-ILMs). The system was homogeneous before polymerization. The copolymer formed is

insoluble in the hydrocarbon medium and precipitates out after about 10 min of polymerization with the reaction mixture becoming noticeably turbid, indicating the formation of colloiddally stable particles. Figure 4 shows SEM images of particles prepared by

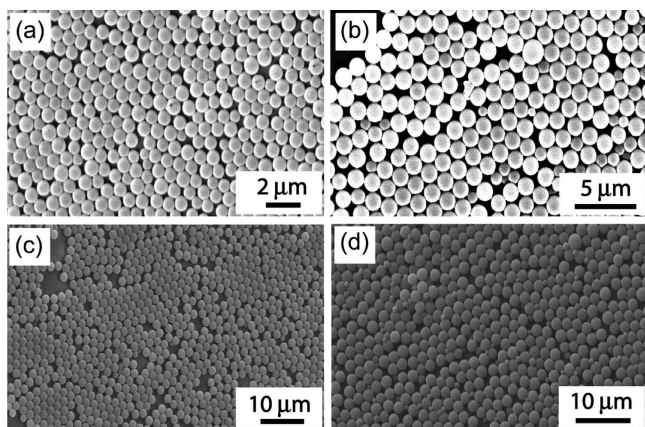


Figure 4. SEM images of poly([ILM-C₁₂][TFPhB]) copolymer particles prepared with (a) 2.0, (b) 4.0, (c) 6.0, and (d) 8.0 wt % ionic monomer as a fraction of the total monomer weight.

dispersion polymerization containing different concentrations of monomer [ILM-C₁₂][TFPhB]. The particles obtained were spherical and micrometer-sized and had a high degree of monodispersity as evidenced by the ~3% value measured for the coefficient of the radius of variation C_v . The size and polydispersity of the particles prepared are listed in Table 4. Increasing the

Table 4. Characterization of Poly(ionic liquid)-Containing Latices

latex	IL-monomer	W_{ILM} (wt %) ^a	a (nm) ^b	a_h (nm) ^c	C_v (%) ^d	dye (10 ⁻² wt %) ^e
L1		0.0	270	345	7	0.00
L2	[ILM-C ₆][TFPhB]	2.0	790	775	5	0.00
L3	[ILM-C ₆][TFPhB]	4.0	1070	855	8	0.00
L4	[ILM-C ₆][TFPhB]	6.0	1250	1265	9	0.00
L5	[ILM-C ₆][TFPhB]	8.0	575	620	8	0.13
L6		0.0	430	475	6	0.13
L7	[ILM-C ₁₂][TFPhB]	2.0	365	440	8	0.13
L8	[ILM-C ₁₂][TFPhB]	4.0	600	655	12	0.13
L9	[ILM-C ₁₂][TFPhB]	6.0	900	925	6	0.13
L10	[ILM-C ₁₂][TFPhB]	8.0	935	985	7	0.13

^aPercentage of ionic liquid monomer as a fraction of the weight of MMA and MAA monomers. ^bAverage radius from SEM. ^cAverage hydrodynamic radius from DLS. ^dCoefficient of radius variation from SEM. ^eFluorescent DiIC₁₈ dye added as a percentage of the total preparation weight.

concentration of either the [ILM-C₆][TFPhB] or [ILM-C₁₂][TFPhB] monomer in the synthesis resulted in an increase in the mean particle radius. This dependence probably reflected the greater solubility of the ILM-containing copolymer in the medium and the consequent delay in precipitation until later in the reaction, at which point the precursor polymer particles have grown significantly larger. However the microstructure and, in particular, the location of the ionic groups within the particles have not been determined. A hydrophobic fluorescent dye (DiIC₁₈, 1,1'-dioctadecyl-3,3',3'-tetramethylindocarbocyanine perchlorate) was incorporated⁵³ into preparations L5–L10 to confirm that model fluorescent particles, suitable for confocal microscopy, could be prepared by this route.

4.4. Surface Potentials of PIL Particles in Low-Polarity

Solvents. Poly(ionic liquid)-functionalized particles, when dispersed in a low-polarity solvent such as dodecane where the concentration of ionic impurities can be robustly controlled, provide a very close experimental approximation to what is probably the simplest theoretical model of a charged colloid, namely, a counterion-only or salt-free system. Free ions are generated only by the dissociation of surface groups and so must have the opposite sign of charge to that of the particles. Furthermore, in the absence of impurities, the concentration of co-ions in solution is negligible. The relatively high ionic dissociation efficiency, which is evident in Figure 2, suggests that our particles will be highly charged and develop large surface potentials. To quantify the magnitude of the surface potential, the motion of PIL-containing microparticles was measured in an electric field. This motion is quantified by the electrophoretic mobility $\mu = v/E$, the ratio of the particle velocity v to the electric field E . The electrophoretic mobility depends on both the potential at the surface of the particle and the concentration of ions in solution through the polarization of the screening cloud that surrounds a charged particle in solution and generates a drag effect as it moves in the opposite direction to the particle as a field is applied. Theoretical studies^{38,39,54–56} have shown that the ion distribution around a spherical charged particle of radius a in a salt-free medium containing only counterions is very different from that present in an electrolyte solution. If the salt concentration c_s is low enough to satisfy the condition $\xi \gg a$, where $\xi = (8\pi\lambda_B c_s)^{-1/2}$ is the Debye length, then a highly charged spherical particle at a finite concentration exerts such a powerful attraction on its counterions that a certain fraction condenses onto the particle. Counterion condensation is much more marked in a low-salt environment and occurs only where $\xi \gg a$. The resulting nonlinear ion distribution around a charged particle has a dramatic effect on the electrophoretic mobility.³⁹ A plot of the mobility as a function of the charge $Z\lambda_B/a$ (or the surface potential Φ_s) grows initially linearly before exhibiting a plateau, at a threshold value of the charge, beyond which μ should become independent of the charge level as counterion collapse onto the surface of the particle is initiated. Consequently, to determine the zeta (or surface) potential properly from the measured electrophoretic mobility, we must solve simultaneously the full coupled nonlinear Poisson–Boltzmann and Navier–Stokes equations. The conventional Hückel result, which assumes linear electrostatics, is increasingly inaccurate at high surface potentials³⁷ as the nonlinear interactions that result in condensation become increasingly significant. To calculate the surface potential from the measured μ , we use the method proposed by Ohshima and outlined in section 3.2. A numerical solution of the Poisson–Boltzmann equation in a salt-free medium is employed together with a single-particle solution of the full electrokinetic equations, valid if the particle volume fraction η_c is sufficiently small,^{37,41,42} to calculate the dependence of μ as a function of $\Phi_s - \Phi_o$. A numerical interpolation routine is then used to evaluate the surface potential from the measured mobility data. In a counterion-only system, the surface potential and ion concentration are no longer independent of each other. Because the ions in solution arise from the dissociation of surface groups, an increase in either the surface charge or the concentration of particles results in an increase in the ion concentration and a subsequent change in μ . Consequently, the mobility μ in a salt-free system will depend strongly on the particle concentration.

The dimensionless electrophoretic mobility μ^* is plotted in Figure 5a as a function of W_{ILM} , the percentage by weight of ionic monomer, for both the C₆ and C₁₂ systems. To ensure that the mobility data reflects the concentration of surface groups and is

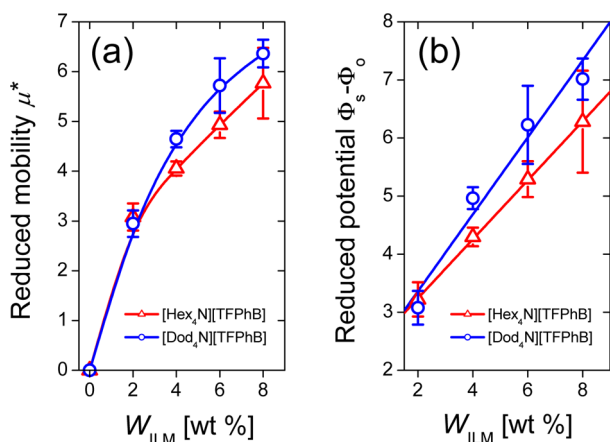


Figure 5. (a) Reduced mobility μ^* and (b) potential difference $\Phi_s - \Phi_o$ between the surface of the particle and the boundary of the WS cell as a function of the weight percent of poly(ionic monomer), W_{ILM} , expressed as a fraction of the total weight of monomer used in the particle synthesis. The solid lines are guides to the eye.

not affected by the particle concentration, all measurements were recorded at a fixed colloid volume fraction of $\eta_c = 3.8 \times 10^{-5}$. The full dependence of the mobility on the concentration of particles will be the subject of a forthcoming paper. Without any poly(ionic liquid) groups, the particles exhibit no response to the applied electric field. Particles with ionic monomer move in the same direction as the applied field, so the particles are positively charged. The mobility increases as the concentration of PIL groups increases although the dependence of μ^* on W_{ILM} is less than linear. As might be expected from the ionic dissociation data, the particles functionalized with C_{12} cations display higher mobilities than those containing C_6 cations. We use this data to calculate the dimensionless potential difference $\Phi_s - \Phi_o$ between the surface of the particle and the cell boundary, which in an interacting system defines the electrophoretic mobility. The results are plotted in Figure 5b. Remarkably, we note that the corresponding potential differences, derived from the solution of the full nonlinear PB equation, are now very close to linear in the fraction of ionic monomer, suggesting that the concentration of charged surface groups is directly proportional to their bulk concentration. The potential differences are surprisingly large with a maximum value for the 8 wt % C_{12} cation of $\Phi_s - \Phi_o = +7.0 \pm 0.4$ or equivalently a potential of 180 ± 9 mV. The high particle charge results in a substantial pair repulsion that is apparent in the strong, long-range ordering that is clearly visible in dilute suspensions with optical microscopy. Preliminary holographic optical tweezers experiments demonstrate the existence of strong electrostatic forces, and more detailed measurements are underway to check the estimates of Φ_s found by electrophoresis. Surface potentials in nonpolar solvents reported in the literature^{8,9,12,14,15} seldom exceed 100 mV and often are appreciably smaller.^{57,58} Indeed, the surface potential of our PIL-functionalized particles is remarkably large even by comparison to that of a highly charged aqueous system.⁵⁹ Taken together, these observations demonstrate that PIL-functionalized particles form a unique model system with strong and adjustable electrostatic interactions in a nonpolar environment.

5. CONCLUSIONS

Polymer particles that develop a large spontaneous charge in a low-polarity solvent were obtained by functionalizing the surface of a poly(methyl methacrylate) particle with ionic liquid groups. The particles were prepared by a straightforward modification of

an already-existing dispersion polymerization, resulting in spherical, highly monodisperse particles with diameters ranging from ~ 50 nm to a few micrometers. A polymerizable ionic liquid monomer was synthesized in which a tetra-alkyl ammonium cation and a tetrakis[3,5-bis(trifluoromethyl) phenyl]borate anion were bridged by a short C_3 alkyl chain to a methacrylate group. A homologous series of monomers were prepared with different alkyl chain lengths (C_4 – C_{18}). The charge on the particle can be varied almost at will by changing the proportion of the ionic liquid monomer copolymerized with methyl methacrylate and methacrylic acid. In contrast to conventional surfactant-based approaches, this new class of colloids represents a nearly perfect approximation to a classical counterion-only charged system. The ability to tune the charge and so control the electrostatic interactions between nonpolar particles offers the opportunity to explore systematically the complex phase diagram of binary superlattice formation^{5,9} and establish the conditions necessary for the self-assembly of new photonic materials.⁶⁰ In addition the ability to define a specific charge state in a mixture of different particles may offer benefits for a new generation of high-resolution electrophoretic displays.

■ ASSOCIATED CONTENT

Supporting Information

NMR and elemental analysis data for all compounds. This material is available free of charge via the Internet at <http://pubs.acs.org/>.

■ AUTHOR INFORMATION

Corresponding Author

*E-mail: p.bartlett@bristol.ac.uk.

Notes

The authors declare no competing financial interest.

■ ACKNOWLEDGMENTS

G.H. thanks the Punjab Educational Endowment Fund for financial support. We thank Dr. N. Greinert of Merck Chemicals Ltd. U.K., an affiliate of Merck KGaA, Darmstadt, Germany, for providing the Na[TFPhB] precursor and for many helpful discussions.

■ REFERENCES

- (1) Walker, D. A.; Kowalczyk, B.; de la Cruz, M. O.; Grzybowski, B. A. Electrostatics at the nanoscale. *Nanoscale* **2011**, *3*, 1316–1344.
- (2) Walker, D. A.; Wilmer, C. E.; Kowalczyk, B.; Bishop, K. J. M.; Grzybowski, B. A. Precision assembly of oppositely and like-charged nanoobjects mediated by charge-induced dipole interactions. *Nano Lett.* **2010**, *10*, 2275–2280.
- (3) Zhou, J.; An, J.; Tang, B.; Xu, S.; Cao, Y.; Zhao, B.; Xu, W.; Chang, J.; Lombardi, J. R. Growth of tetrahedral silver nanocrystals in aqueous solution and their SERS enhancement. *Langmuir* **2008**, *24*, 10407–10413.
- (4) de Graaf, J.; Boon, N.; Dijkstra, M.; van Roij, R. Electrostatic interactions between Janus particles. *J. Chem. Phys.* **2012**, *137*, 104910–12.
- (5) Leunissen, M. E.; Christova, C. G.; Hynninen, A. P.; Royall, C. P.; Campbell, A. I.; Imhof, A.; Dijkstra, M.; van Roij, R.; van Blaaderen, A. Ionic colloidal crystals of oppositely charged particles. *Nature* **2005**, *437*, 235–240.
- (6) Smallenburg, F.; Boon, N.; Kater, M.; Dijkstra, M.; van Roij, R. Phase diagrams of colloidal spheres with a constant zeta-potential. *J. Chem. Phys.* **2011**, *134*, 074505–8.

- (7) de Graaf, J.; Zwanikken, J.; Bier, M.; Baarsma, A.; Oloumi, Y.; Spelt, M.; van Roij, R. Spontaneous charging and crystallization of water droplets in oil. *J. Chem. Phys.* **2008**, *129*.
- (8) Merrill, J. W.; Sainis, S. K.; Dufresne, E. R. Many-body electrostatic forces between colloidal particles at vanishing ionic strength. *Phys. Rev. Lett.* **2009**, *103*, 138301.
- (9) Roberts, G. S.; Sanchez, R.; Kemp, R.; Wood, T.; Bartlett, P. Electrostatic charging of nonpolar colloids by reverse micelles. *Langmuir* **2008**, *24*, 6530–6541.
- (10) Leunissen, M. E.; van Blaaderen, A.; Hollingsworth, A. D.; Sullivan, M. T.; Chaikin, P. M. Electrostatics at the oil-water interface, stability, and order in emulsions and colloids. *Proc. Natl. Acad. Sci. U.S.A.* **2007**, *104*, 2585–2590.
- (11) Hsu, M. F.; Dufresne, E. R.; Weitz, D. A. Charge stabilization in nonpolar solvents. *Langmuir* **2005**, *21*, 4881–4887.
- (12) Guo, Q.; Lee, J.; Singh, V.; Behrens, S. H. Surfactant mediated charging of polymer particles in a nonpolar liquid. *J. Colloid Interface Sci.* **2013**, *392*, 83–89.
- (13) Huiying, C.; Yongjian, C.; Pinwen, H.; Ming, Q. Investigation of charging behavior of PS particles in nonpolar solvents. *Nanotechnology* **2011**, *22*, 445709.
- (14) Kemp, R.; Sanchez, R.; Mutch, K. J.; Bartlett, P. Nanoparticle charge control in nonpolar liquids: insights from small-angle neutron scattering and microelectrophoresis. *Langmuir* **2010**, *26*, 6967–6976.
- (15) Poovarodom, S.; Berg, J. C. Effect of particle and surfactant acid-base properties on charging of colloids in apolar media. *J. Colloid Interface Sci.* **2010**, *346*, 370–377.
- (16) Guo, Q.; Singh, V.; Behrens, S. H. Electric charging in nonpolar liquids because of nonionizable surfactants. *Langmuir* **2010**, *26*, 3203–3207.
- (17) Hashmi, S. M.; Firoozabadi, A. Field- and concentration-dependence of electrostatics in nonpolar colloidal asphaltene suspensions. *Soft Matter* **2012**, *8*, 1878–1883.
- (18) Hashmi, S. M.; Firoozabadi, A. Tuning size and electrostatics in non-polar colloidal asphaltene suspensions by polymeric adsorption. *Soft Matter* **2011**, *7*, 8384–8391.
- (19) Morrison, I. D. Electrical charges in nonaqueous media. *Colloids Surf.* **1993**, *71*, 1–37.
- (20) Mecerreyes, D. Polymeric ionic liquids: broadening the properties and applications of polyelectrolytes. *Prog. Polym. Sci.* **2011**, *36*, 1629–1648.
- (21) Yuan, J.; Antonietti, M. Poly(ionic liquid)s: polymers expanding classical property profiles. *Polymer* **2011**, *52*, 1469–1482.
- (22) Armand, M.; Endres, F.; MacFarlane, D. R.; Ohno, H.; Scrosati, B. Ionic-liquid materials for the electrochemical challenges of the future. *Nat. Mater.* **2009**, *8*, 621–629.
- (23) Ohno, H. Design of ion conductive polymers based on ionic liquids. *Macromol. Symp.* **2007**, *249–250*, 551–556.
- (24) Neouze, M. A. About the interactions between nanoparticles and imidazolium moieties: emergence of original hybrid materials. *J. Mater. Chem.* **2010**, *20*, 9593–9607.
- (25) Zhang, H.; Cui, H. Synthesis and characterization of functionalized ionic liquid-stabilized metal (gold and platinum) nanoparticles and metal nanoparticle/carbon nanotube hybrids. *Langmuir* **2009**, *25*, 2604–2612.
- (26) Wilke, A.; Yuan, J.; Antonietti, M.; Weber, J. Enhanced carbon dioxide adsorption by a mesoporous poly(ionic liquid). *ACS Macro Lett.* **2012**, *1*, 1028–1031.
- (27) Sanchez, R.; Bartlett, P. Synthesis of charged particles in an ultra-low dielectric solvent. *Soft Matter* **2011**, *7*, 887–890.
- (28) Abbott, A. P.; Griffith, G. A.; Harper, J. C. Conductivity of long chain quaternary ammonium electrolytes in cyclohexane. *J. Chem. Soc. Faraday Trans.* **1997**, *93*, 577–582.
- (29) Menshutkin, N. Über die Affinitätskoeffizienten der Alkylhaloide und der Alkylhaloide und der Amine. *Z. Phys. Chem.* **1890**, *6*, 41–57.
- (30) Jiang, Y.-L.; Hu, Y.-Q.; Pang, J.; Yuan, Y.-C. Syntheses of long-chain quaternary ammonium salts from fatty alcohols by microwave irradiation. *J. Am. Oil Chem. Soc.* **1996**, *73*, 847–850.
- (31) Antl, L.; Goodwin, J. W.; Hill, R. D.; Ottewill, R. H.; Owens, S. M.; Papworth, S.; Waters, J. A. The preparation of poly(methyl methacrylate) latices in non-aqueous media. *Colloids Surf.* **1986**, *17*, 67–78.
- (32) Marcus, Y.; Hefter, G. Ion pairing. *Chem. Rev.* **2006**, *106*, 4585–4621.
- (33) Valeriani, C.; Camp, P. J.; Zwanikken, J. W.; van Roij, R.; Dijkstra, M. Ion association in low-polarity solvents: comparisons between theory, simulation, and experiment. *Soft Matter* **2010**, *6*, 2793–2800.
- (34) Marcus, Y. Tetraalkylammonium ions in aqueous and non-aqueous solutions. *J. Solution Chem.* **2008**, *37*, 1071–1098.
- (35) van Roij, R. Electrostatics in liquids: from electrolytes and suspensions towards emulsions and patchy surfaces. *Phys. A* **2010**, *389*, 4317–4331.
- (36) Russel, W. B.; Saville, D. A.; Schowalter, W. R. *Colloidal Dispersions*; Cambridge University Press: Cambridge, U.K., 1989.
- (37) Ohshima, H. Numerical calculation of the electrophoretic mobility of a spherical particle in a salt-free medium. *J. Colloid Interface Sci.* **2003**, *262*, 294–297.
- (38) Ohshima, H. Surface charge density/surface potential relationship for a spherical colloidal particle in a salt-free medium. *J. Colloid Interface Sci.* **2002**, *247*, 18–23.
- (39) Ohshima, H. Electrophoretic mobility of a spherical colloidal particle in a salt-free medium. *J. Colloid Interface Sci.* **2002**, *248*, 499–503.
- (40) Lobaskin, V.; Duenweg, B.; Medebach, M.; Palberg, T.; Holm, C. Electrophoresis of colloidal dispersions in the low-salt regime. *Phys. Rev. Lett.* **2007**, *98*, 176105.
- (41) Carrique, F.; Ruiz-Reina, E.; Arroyo, F. J.; Delgado, A. V. Cell Model of the direct current electrokinetics in salt-free concentrated suspensions: the role of boundary conditions. *J. Phys. Chem. B* **2006**, *110*, 18313–18323.
- (42) Chiang, C.-P.; Lee, E.; He, Y.-Y.; Hsu, J.-P. Electrophoresis of a spherical dispersion of polyelectrolytes in a salt-free solution. *J. Phys. Chem. B* **2006**, *110*, 1490–1498.
- (43) Alexander, S.; Chaikin, P. M.; Grant, P.; Morales, G. J.; Pincus, P.; Hone, D. Charge renormalization, osmotic pressure, and bulk modulus of colloidal crystals: theory. *J. Chem. Phys.* **1984**, *80*, 5776–5781.
- (44) Trizac, E.; Bocquet, L.; Aubouy, M.; von Grunberg, H. H. Alexander's prescription for colloidal charge renormalization. *Langmuir* **2003**, *19*, 4027–4033.
- (45) Ohshima, H. Electrophoresis of colloidal particles in a salt-free medium. *Chem. Eng. Sci.* **2006**, *61*, 2104–2107.
- (46) Giupponi, G.; Pagonabarraga, I. Colloid electrophoresis for strong and weak ion diffusivity. *Phys. Rev. Lett.* **2011**, *106*, 248304–248304.
- (47) Yoshizawa, M.; Ohno, H. Molecular brush having molten salt domain for fast ion conduction. *Chem. Lett.* **1999**, *28*, 889–890.
- (48) Abbott, A. P.; Claxton, T. A.; Fawcett, J.; Harper, J. C. Tetrakis(decyl)ammonium tetraphenylborate: a novel electrolyte for non-polar media. *J. Chem. Soc., Faraday Trans.* **1996**, *92*, 1747–1749.
- (49) Tamaki, K. The surface activity of tetra-n-alkylammonium halides in aqueous solutions. The effect of hydrophobic hydration. *Bull. Chem. Soc. Jpn.* **1974**, *47*, 2764–2767.
- (50) Eicke, H. F.; Borkovec, M.; Das-Gupta, B. Conductivity of water-in-oil microemulsions: a quantitative charge fluctuation model. *J. Phys. Chem.* **1989**, *93*, 314–317.
- (51) Atkins, P.; de Paula, J. *Atkins' Physical Chemistry*, 9th ed.; Oxford University Press: Oxford, U.K., 2010.
- (52) Ogihara, W.; Washiro, S.; Nakajima, H.; Ohno, H. Effect of cation structure on the electrochemical and thermal properties of ion conductive polymers obtained from polymerizable ionic liquids. *Electrochim. Acta* **2006**, *51*, 2614–2619.
- (53) Campbell, A. I.; Bartlett, P. Fluorescent hard-sphere polymer colloids for confocal microscopy. *J. Colloid Interface Sci.* **2002**, *256*, 325–330.
- (54) Imai, N.; Oosawa, F. Counterion distribution around a highly charged spherical polyelectrolyte. *Busseiron Kenkyu* **1952**, *52*, 42–63.
- (55) Zimm, B. H.; Le Bret, M. Counter-ion condensation and system dimensionality. *J. Biomol. Struct. Dyn.* **1983**, *1*, 461–71.

(56) Manning, G. S. Counterion condensation on charged spheres, cylinders, and planes. *J. Phys. Chem. B* **2007**, *111*, 8554–8559.

(57) Patel, M. N.; Smith, P. G.; Kim, J.; Milner, T. E.; Johnston, K. P. Electrophoretic mobility of concentrated carbon black dispersions in a low-permittivity solvent by optical coherence tomography. *J. Colloid Interface Sci.* **2010**, *345*, 194–199.

(58) Smith, P. G.; Patel, M. N.; Kim, J.; Milner, T. E.; Johnston, K. P. Effect of surface hydrophilicity on charging mechanism of colloids in low-permittivity solvents. *J. Phys. Chem. C* **2007**, *111*, 840–848.

(59) Crocker, J. C.; Grier, D. G. When like charges attract: the effects of geometrical confinement on long-range colloidal interactions. *Phys. Rev. Lett.* **1996**, *77*, 1897–1900.

(60) Hynninen, A. P.; Thijssen, J. H. J.; Vermolen, E. C. M.; Dijkstra, M.; Van Blaaderen, A. Self assembly route for photonic crystals with a bandgap in the visible region. *Nat. Mater.* **2007**, *6*, 202–205.